How to Cite: Valiulina, L.I., Cherepanov, V.N., & Valiev, R.R. (2023). Relationship between the Electric Polarizability and Aromaticity of Metallocene-Containing Macrocycles. *Eurasian Journal of Chemistry, 111(3), 52-59.* https://doi.org/10.31489/2959-0663/3-23-10

Article

Received: 18 May 2023 | Revised: 15 June 2023 | Accepted: 30 June 2023 | Published online: 26 July 2023

UDC 544.032.5+ 537.635

https://doi.org/10.31489/2959-0663/3-23-10

Lenara I. Valiulina, Victor N. Cherepanov, Rashid R. Valiev*

National Research Tomsk State University, Tomsk, Russia
(Corresponding author's e-mail: valievrashid@mail.ru)

Relationship between the Electric Polarizability and Aromaticity of Metallocene-Containing Macrocycles

Magnetically induced ring currents, aromaticity, as well as polarizability and second hyperpolarizability of the metallocenothiaporphyrins with transition metals of group VIII (Fe, Ru) and isoelectronic cations of group IX (Co^+, Rh^+) and metallocene-containing annulenes (($C_5H_5)_2M$[n = 18–24], where M is Fe, Co^+) have been studied computationally at Density Functional level of Theory (DFT). The calculations show that the value of average polarizability of the studied compounds depends on their character of the aromaticity. Aromatic structures are characterized by larger polarizability than their corresponding antiaromatic congeners. The average polarizability of metallocenothiaporphyrins also depends on the magnitude of magnetically induced ring currents, which quantify the degree of electron delocalization. An increase in the number of π-electrons in conjugation pathway plays a key role in the growth of polarizability. Aromaticity also influences on the second hyperpolarizability of metallocene-containing annulenes. In the case of compounds with the same number of conjugated electrons, the second hyperpolarizability is larger for more aromatic systems. To conclude, our results pinpoint the importance of electron delocalization on the polarizability and second hyperpolarizability of the studied metallocene-containig macrocycles.

Keywords: magnetically induced ring currents, aromaticity, polarizability, hyperpolarizability, metallocenothiaporphyrins, optical properties, metallocenes, electron delocalization.

Introduction

The polarizability as well as the first and second hyperpolarizabilities are important optical quantities in the field of chemistry and physics. These characteristics describe the responses of a molecular system when it interacts with an external electric field. Polarizability plays an important role in determining intramolecular and intermolecular interactions, reactivity, and optical properties of materials [1–3]. The values of the first and second hyperpolarizabilities describe nonlinear processes occurring in compounds under the action of intense laser radiation. These processes include second and third harmonic generations, two-photon absorption, the Kerr effect, spontaneous and stimulated Raman scattering [4–7]. The search for molecules with a large nonlinear response is an urgent task, since they are used as molecular electronic, optical limiting devices, molecular switches, as well as sensitizers for photodynamic therapy [8–11].

The polarizability is strongly affected by the presence of conjugated bonds in the molecule [12]. When bond conjugation forms a closed circuit, the electron delocalization occurs, which causes the aromaticity. Aromaticity and electron delocalization determine the specific structural, magnetic, energetic and electronic properties of conjugated systems, which in turn affect the optical and nonlinear optical properties of molecules [13–15]. Thus, macrocyclic aromatic compounds with well-defined electron delocalization present the greatest interest in the study of optical and nonlinear optical properties. Among macrocyclic aromatic systems, metal porphyrin complexes have attracted considerable attention in the last decade due to their exceptional properties [16, 17]. Recent studies have shown that metallocene fragments with Fe and Ru incorporated in the porphyrin circuit are able to transfer π-conjugation [18, 19]. The transmission of π-electron conjugation across a *d*-electron metallocene contributes to three-dimensional metallomacrocyclic aromaticity [20]. The metallocene fragment in the porphyrin leads to a unique electronic structure, which can be reflected in special photophysical and electronic properties, aromaticity, conformational flexibility, as well as non-linear optical properties.

In this regard, the purpose of this work was a quantum-chemical study of the optical properties of metallocene-containing macrocyclic molecules, an assessment of the effect of conjugation and electron delocalization on optical and nonlinear optical properties. It is important to understand the role of the electronic

structure and electron delocalization in determining optical and nonlinear optical properties for the development of new promising materials.

Computational Details

The molecular structures of the studied metallocenothiaporphyrins are shown in Figure 1. We have investigated metallocenothiaporphyrins with transition metals of group VIII (Fe, Ru) and isoelectronic cations of group IX (Co^+, Rh^+). We denote the studied molecules as $(C_5H_5)_2MP$ for metallocenothiaporphyrins and H_2-$(C_5H_5)_2MP$ for dihydrometallocenothiaporphyrins (Fig. 1). In this notation, M is a metal atom or ion and P is a porphyrin ring.

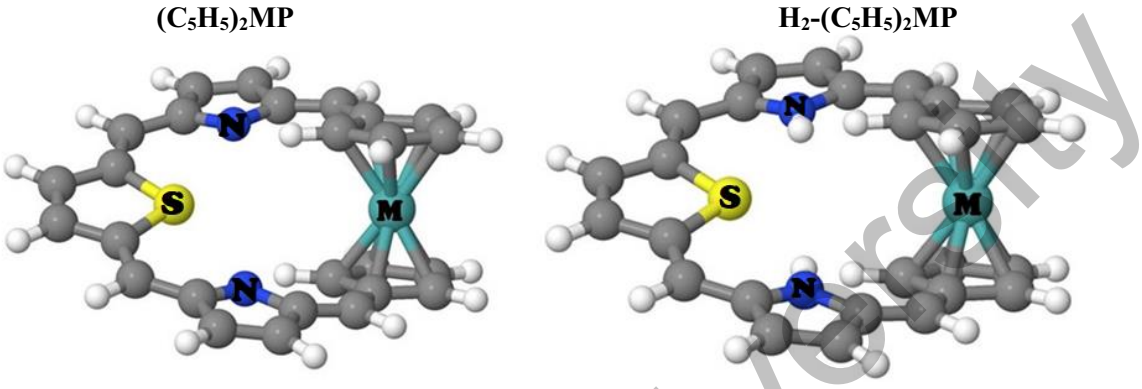

Figure 1. The molecular structures of metallocenothiaporphyrins, where M = Fe, Co^+, Ru, Rh^+

To unravel the effect of conjugation on the optical properties we have considered the hypothetical structures of annulenes with an incorporated metallocene fragment: $(C_5H_5)_2M[n = 18–24]$ (M = Fe, Co^+). The molecular structure of these compounds is shown in Figure 2.

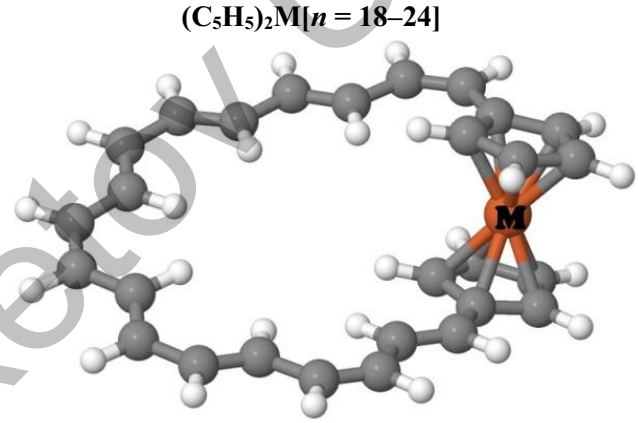

Figure 2. The molecular structure of metalloceno[*n*]anullenes (*n* = 18-24), where M = Fe, Co^+

The optimized structures of the studied molecules were obtained at the density functional theory (DFT) level using the Becke, Lee, Yang, Parr (B3LYP) [21, 22] functional and the Karlsruhe def2-TZVP basis set [23]. The vibrational frequency calculations indicate that all structures are minima on the potential energy surface. The nuclear magnetic shielding tensors, as well as the polarizabilities, and the second hyperpolarizabilities were calculated at the same level of theory. Time-dependent DFT (TD-DFT) calculations were carried out at the B3LYP/def2-TZVP level of theory to evaluate excitation energies and the corresponding oscillator strengths (f) of main low-energy electronic transitions. All calculations were carried out in the quantum-chemical software package GAUSSIAN 9 [24] on the SKIF Cyberia computing cluster.

Calculations of magnetically induced current densities were carried out using the GIMIC method [25], which uses the first-order magnetically perturbed density matrices, unperturbed density matrices and information on the basis set. To get detailed information about the GIMIC program and its capabilities we refer

the reader to [25, 26]. The ring-current strengths (*n*A/T) were obtained by numerically integrating the current density flux passing through the plane placed perpendicularly to the chemical bond.

The average polarizability $\bar{\alpha}$ was obtained by the trace of the polarizability tensor:

$$\bar{\alpha} = \frac{1}{3} tr(\alpha_{ii}) = \frac{1}{3} \sum_{i=x,y,z} \alpha_{ii} \quad (1)$$

and its anisotropy $\Delta\alpha$, defined as:

$$\Delta\alpha^2 = \frac{1}{2}\left[(\alpha_{xx} - \alpha_{yy})^2 + (\alpha_{xx} - \alpha_{zz})^2 + (\alpha_{yy} - \alpha_{zz})^2 + +6\alpha_{xz}{}^2 + 6\alpha_{xy}{}^2 + 6\alpha_{yz}{}^2\right]. \quad (2)$$

The parallel component of average second hyperpolarizability $\gamma_{//}$ was defined as:

$$\gamma_{//}(-2\omega; \omega, \omega, 0) = \frac{1}{15} \sum_{i,j=x,y,z} (\gamma_{iijj} + \gamma_{ijij} + \gamma_{ijji}). \quad (3)$$

Results and Discussion

Polarizability of metallocenothiaporphyrins

The ring-current strengths, aromaticity and the average polarizabilities of the studied metallocenothiaporphyrins are summarized in Table 1. The results of the ring-current strengths were taken from our previous works [20].

Table 1

Magnetically induced ring-current strength *I*, aromaticity and the average polarizability $\bar{\alpha}$ and its anisotropy $\Delta\alpha$ computed at different frequencies (ω, eV) of the studied metallocenothiaporphyrins

Molecule	*I*, *n*A/T	$\Delta E_{\text{HOMO-LUMO}}$, eV	$\bar{\alpha}$, a.u./$\Delta\alpha$, a.u.			
			0, eV	0.544, eV	0.653, eV	1.034, eV
$(C_5H_5)_2FeP$	–10.4 (ant.)	1.97	419/292	424/299	427/302	444/325
H_2-$(C_5H_5)_2FeP$	13.8 (ar.)	2.19	447/331	454/339	456/343	473/366
$(C_5H_5)_2RuP$	–10.8 (ant.)	1.96	428/284	433/290	435/294	451/315
H_2-$(C_5H_5)_2RuP$	15.3 (ar.)	2.21	460/331	466/339	469/343	485/366
$(C_5H_5)_2Co^+P$	–21.3 (ant.)	1.66	410/285	417/294	420/298	-932/3939*
H_2-$(C_5H_5)_2Co^+P$	21.8 (ar.)	2.22	455/349	461/358	464/362	483/387
$(C_5H_5)_2Rh^+P$	–20.5 (ant.)	1.71	420/279	426/287	430/291	482/386
H_2-$(C_5H_5)_2Rh^+P$	23.2 (ar.)	2.24	466/348	473/357	476/361	493/384

* The negative value of polarizability indicates that the field frequency is higher than the frequency corresponding to the transition to the first excited state ($\Delta E(S_0 \rightarrow S_1)$ = 1.03 eV)

The result of the calculations showed that antiaromatic systems are characterized by a smaller energy gap between the frontier molecular orbitals $\Delta E_{\text{HOMO-LUMO}}$ compared to their aromatic counterparts. The value of energy gap determines the chemical stability of the compounds, so the low $\Delta E_{\text{HOMO-LUMO}}$ values for antiaromatic molecules explain their high reactivity [27]. The energy gap also affects the optical properties. So, molecules must have a small energy gap to obtain high values of polarizability [28]. In simple perturbation theory when the two-level model is used polarizability can be obtained by [2]:

$$\alpha \approx \frac{\mu_t{}^2}{E_{HOMO-LUMO}}, \quad (4)$$

where μ_t —the transition dipole moment from the ground state to the first dipole-allowed excited state. $\alpha \sim \frac{1}{\Delta E_{\text{HOMO-LUMO}}}$

However, the analysis of Table 1 shows that the average polarizability of aromatic systems, despite the large energy gap, is larger than for corresponding antiaromatic congeners both in the static and dynamic regimes (Fig. 3). The average polarizability increases in the following order: $(C_5H_5)_2Co^+P$ < $(C_5H_5)_2FeP$ < $(C_5H_5)_2Rh^+P$ < $(C_5H_5)_2RuP$ for antiaromatic metallocenothiaporphyrins and H_2-$(C_5H_5)_2FeP$ < H_2-$(C_5H_5)_2Co^+P$ < H_2-$(C_5H_5)_2RuP$ < H_2-$(C_5H_5)_2Rh^+P$ for aromatic metallocenothiaporphyrins. Compounds with 3*d* metals (Fe, $Co^{+)}$ have lower average polarizability values, which is caused by the stronger binding of electrons to the nucleus.

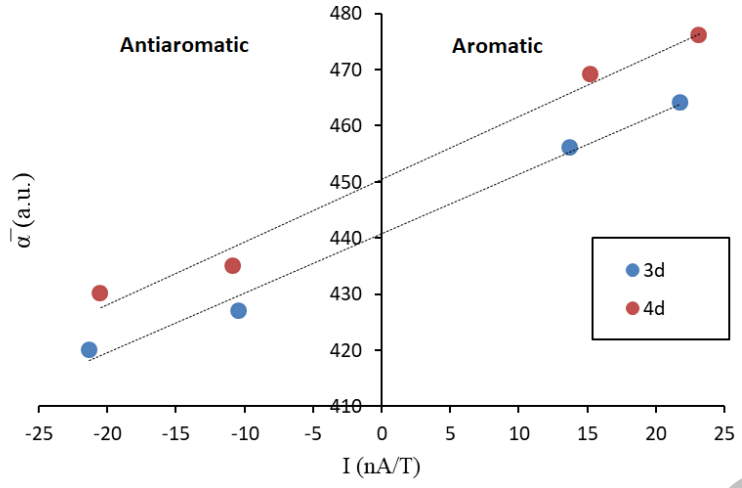

Figure 3. Average polarizability $\bar{\alpha}$ ($\omega = 0.653$ eV) as a function of ring-current strength for the studied metallocenothiaporphyrins

Eq. (4) can be modified in terms of oscillator strength to [29]:

$$\alpha = \frac{\hbar^2 e^2}{m_e} \sum_{l \neq k} \frac{f_{kl}}{\Delta E_{kl}^{\ 2}}, \tag{5}$$

where the summation runs over all integrals including the continuum.

Eq. (5) implies that the large contributions to the polarizability come from low-lying high intensity electronic transitions. In general, aromatic compounds characterized by distinctive absorption, whereas antiaromatic species show smeared and attenuated absorption bands [30]. Moreover, the low-lying electronic transition ($S_0 \rightarrow S_1$) corresponding to HOMO→LUMO transition in antiaromatic porphyrinoids is optically forbidden while in aromatic molecules this transition forms Q-bands in the absorption spectra [31]. Table 2 presents the characteristic properties of the first and the main optically-allowed electronic transitions ($f > 0.01$) of the studied metallocenothiaporphyrins.

Table 2

Vertical excitation energies of the first and the main electronic transitions of the studied metallocenothiaporphyrins

Antiaromatic			Aromatic			Antiaromatic			Aromatic		
$S_0 \rightarrow S_n$	E, eV	f	$S_0 \rightarrow S_n$	E, eV	f	$S_0 \rightarrow S_n$	E, eV	f	$S_0 \rightarrow S_n$	E, eV	f
$(C_5H_5)_2FeP$			H_2-$(C_5H_5)_2FeP$			$(C_5H_5)_2Co^+P$			H_2-$(C_5H_5)_2Co^+P$		
S_1	1.24	0.004	S_1	1.77	0.050	S_1	1.03	0.008	S_1	1.51	0.020
S_3	1.68	0.030	S_3	2.07	0.070	S_2	1.95	0.014	S_4	2.28	0.013
S_{10}	2.93	0.014	S_5	2.30	0.020	S_3	2.27	0.012	S_5	2.32	0.040
			S_7	2.64	0.014	S_4	2.32	0.020	S_6	2.59	0.110
			S_9	2.74	0.030	S_7	2.55	0.030	S_7	2.63	0.060
			S_{10}	2.91	0.028	S_{10}	2.68	0.040	S_9	2.86	0.270
									S_{10}	2.96	0.300
$(C_5H_5)_2RuP$			H_2-$(C_5H_5)_2RuP$			$(C_5H_5)_2Rh^+P$			H_2-$(C_5H_5)_2Rh^+P$		
S_1	1.39	0.016	S_1	1.92	0.110	S_1	1.11	0.010	S_1	1.78	0.043
S_3	2.07	0.020	S_5	2.89	0.200	S_2	2.24	0.030	S_4	2.78	0.200
S_4	2.12	0.010	S_6	3.05	0.250	S_8	2.83	0.100	S_5	2.93	0.500
S_5	2.60	0.050	S_7	3.07	0.300	S_9	3.05	0.010	S_6	2.97	0.400
S_6	2.88	0.020	S_8	3.29	0.060	S_{10}	3.08	0.350	S_7	3.40	0.400
S_7	2.92	0.050	S_9	3.31	0.500				S_8	3.52	0.030
S_{10}	3.03	0.200	S_{10}	3.39	0.020				S_9	3.61	0.020

As can be seen from the Table 2 the number of optically allowed transitions in the aromatic structures of metallocenothiaporphyrins in general is greater than in antiaromatic ones. Moreover, these transitions are

more intense. This explains why aromatic metallocenothiaporphyrins have larger polarizability than antiaromatic metallocenothiaporphyrins.

Figure 3 illustrates that, beside the aromaticity effect, the average polarizability in metallocenothiaporphyrins depends on the magnetically induced ring-currents strength I (nA/T), which determines the degree of electron delocalization.

It should be noted that we calculated the magnetic susceptibility for the $(C_5H_5)_2Co^+P$ molecule. The result shows that $(C_5H_5)_2Co^+P$ is diamagnetic ($\chi = -13.2$ a.u.). The diamagnetic character as well as the negative average polarizability at 1.034 eV ($\bar{\alpha} = -932$ a.u.), indicate that $(C_5H_5)_2Co^+P$ can potentially be used as a building block for advanced optical materials with a negative refractive index [32].

Polarizability and Second hyperpolarizability of metallocene-containing annulenes

The ring-current strengths, aromaticity and the average polarizabilities of the studied metallocene-containing annulenes are presented on Table 3.

Table 3

Magnetically induced ring-current strength *I*, aromaticity and the average polarizability $\bar{\alpha}$ and its anisotropy $\Delta\alpha$ computed at different frequencies (ω, eV) of the studied metalloceno[*n*]anullenes (*n* = 18–24)

Molecule	*I*, *n*A/T	$\Delta E_{HOMO-LUMO}$, eV	$\bar{\alpha}$, a.u./ $\Delta\alpha$, a.u.			
			0, eV	0.544, eV	0.653, eV	1.034, eV
$(C_5H_5)_2Fe$[18]	–5.5(ant.)	2.13	493/423	500/434	504/439	523/466
$(C_5H_5)_2Fe$[20]	5.3(ar.)	2.16	577/503	587/519	593/526	622/566
$(C_5H_5)_2Fe$[22]	–2.8 (non.)	1.97	635/586	649/605	656/614	696/669
$(C_5H_5)_2Fe$[24]	2.8 (non.)	1.98	757/730	781/763	793/780	879/898
$(C_5H_5)_2Co^+$[18]	–16.1(ant.)	1.62	511/463	520/477	524/484	524/517
$(C_5H_5)_2Co^+$[20]	17.6(ar.)	1.92	628/591	644/614	652/626	698/696
$(C_5H_5)_2Co^+$[22]	–18.4(ant.)	1.43	658/622	673/644	680/654	711/706
$(C_5H_5)_2Co^+$[24]	16.8(ar.)	1.72	798/801	827/846	842/869	943/1029

The ring current calculations reveals that metalloceno[*n*]anullenes (*n* = 18–24) with Fe, in contrast to Co+, have less effective conjugation and weakly pronounced electron delocalization, which is confirmed by weak ring-current strengths. This indicates that the charge in the system is involved in the electron delocalization, leading to its enhancement. Molecules $(C_5H_5)_2Fe$[*n* = 22] and $(C_5H_5)_2Fe$[*n* = 24] are non-aromatic (|*I*|<3 *n*A/T). The nonaromatic character of these systems is also confirmed by the energy gap $\Delta E_{HOMO-LUMO}$. For compounds with Fe, $\Delta E_{HOMO-LUMO}$ does not change significantly with a change in the number of π-electrons, while for compounds with Co^+, the energy gap increases for aromatic systems and decreases for antiaromatic ones.

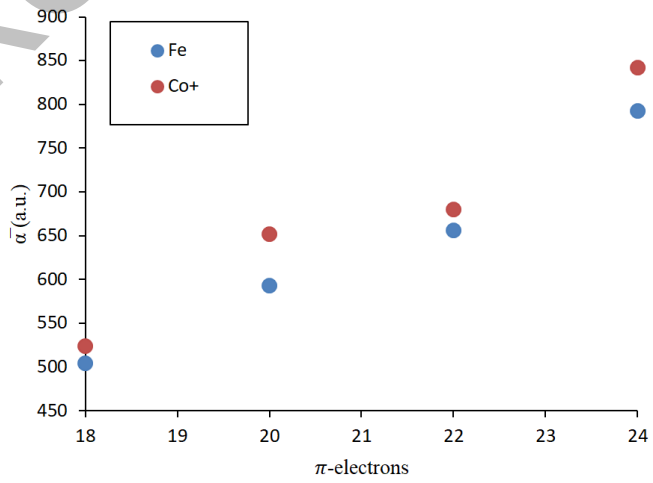

Figure 4. Average polarizability $\bar{\alpha}$ (ω = 0.653 eV) as a function of π- electrons for the studied metalloceno[*n*]anullenes (*n* = 18–24)

The polarizability of the investigated metalloceno[n]anullenes (n = 18–24) increases with an increase in the number of π-electrons (Fig. 4). Structures with Co^+ have the larger average polarizabilities. The greater difference in values between metalloceno[18–24]anullenes with Co^+ and Fe is observed for the aromatic systems $(C_5H_5)_2Co^+[n = 20]$ and $(C_5H_5)_2Co^+[n = 24]$. Thus, for isoelectronic systems the aromatic properties lead to increase the polarizability values.

The results of the parallel component of average second hyperpolarizability calculations for the investigated metalloceno[n]anullenes (n = 18–24) are presented in Table 4.

Table 4

Second Hyperpolarizabilities $\gamma_{//}$ at ω=0.653 eV of the studied metalloceno[18–24]anullenes

Molecule	I, nA/T	$\gamma_{//}$, 10^3 a.u.
$(C_5H_5)_2Fe[n = 18]$	–5.5(ant.)	1150
$(C_5H_5)_2Fe[n = 20]$	5.3(ar.)	1860
$(C_5H_5)_2Co^+[n = 18]$	–16.1(ant.)	1488
$(C_5H_5)_2Co^+[n = 20]$	17.6(ar.)	17053

Table 4 shows that the second hyperpolarizability $\gamma_{//}$ is greater for aromatic systems. Moreover, the character of the aromaticity, as well as its degree plays an important role, which is expressed through the strength of magnetically induced currents. Thus, the more aromatic structure $(C_5H_5)_2Co^+[n = 20]$ has the second hyperpolarizability in order of magnitude higher than the one for the less aromatic structure $(C_5H_5)_2Fe[n = 20]$.

Conclusions

Magnetically induced ring currents, polarizability and second hyperpolarizability for metallocene-containing macrocyclic molecules were studied by means of density functional theory (B3LYP/def2-TZVP) calculations. The calculations results showed that the aromatic character and the number of conjugated electrons in the structure are the key factors leading to an increase in the polarizability of the studied molecules. Moreover, the average polarizability of metallocenothiaporphyrins also depends on the magnetically induced ring-current strengths, which determines the degree of electron delocalization and aromaticity. It was also shown that the average polarizability grows linearly on going from antiaromatic to aromatic metallocenothiaporphyrins molecules. The obtained results demonstrate that the studied metallocene-containing macrocycles are promising molecules with special structure, aromatic and optical properties. Thus, they can be used as nonlinear optical materials.

Acknowledgments

The work was supported by the Foundation for the Advancement of Theoretical Physics and Mathematics “BASIS”. We acknowledge computational resource SKIF Cyberia.

References

1 Hunter, C.A. (2004). Quantifying Intermolecular Interactions: Guidelines for the Molecular Recognition Toolbox. *Angew. Chem. Int. Ed.*, *43*, 5310–5324. https://doi.org/10.1002/anie.200301739

2 Li, X.-D., Wang, H.-Y., Lv, R., Wu, W.-D., Luo, J.-Sh. & Tang, Y.-J. (2009). Correlations of the Stability, Static Dipole Polarizabilities, and Electronic Properties of Yttrium Clusters. *J. Phys. Chem. A*, *113*, 10335–10342. https://doi.org/10.1021/jp904420z

3 Kuznetsova, O.V., Egorochkin, A.N., Khamaletdinova, N.M. & Domratcheva-Lvova, L.G. (2015). Reactivity of Organometallic Compounds and Polarizability Effect. *Journal of Organometallic Chemistry, 779*, 73-80. https://doi.org/10.1016/j.jorganchem.2014.12.004

4 Torres-Torres, C. & García-Beltrán, G. (2022). Study on Second- and Third-Order Nonlinear Optical Properties in Nanostructured Systems: Nanocrystals and Complex Geometries. *Optical Nonlinearities in Nanostructured Systems. Springer Tracts in Modern Physics, 287*, 125–151. https://doi.org/10.1007/978-3-031-10824-2_6

5 Béjot, P., Cormier, E., Hertz, E., Lavorel, B., Kasparian, J., Wolf, J.P. & Faucher, O. (2013). High-field Quantum Calculation Reveals Time-Dependent Negative Kerr Contribution. *Phys. Rev. Lett., 110*, 043902. DOI: 10.1103/PhysRevLett.110.043902

6 Prince, R.C., Frontiera, R.R. & Potma, O. (2017). Stimulated Raman Scattering: From Bulk to Nano. *Chem. Rev., 117*, 5070−5094. https://doi.org/10.1021/acs.chemrev.6b00545

7 Pawlicki, M., Collins, H.A., Denning, R.G. & Anderson, H.L. (2009). Two-Photon Absorption and the Design of Two-Photon Dyes. *Angew. Chem. Int. Ed., 48,* 3244–3266. https://doi.org/10.1002/anie.200805257

8 Lacroix, P.G., Malfant, I. & Lepetit, C. (2016). Second-Order Nonlinear Optics in Coordination Chemistry: an Open Door Towards Multifunctional Materials and Molecular Switches. *Coord. Chem. Rev., 308*, 381−394. https://doi.org/10.1016/j.ccr.2015.05.015

9 Okuno, K., Shigeta, Y., Kishi, R. & Nakano, M. (2013). Photochromic Switching of Diradical Character: Design of Efficient Nonlinear Optical Switches. *J. Phys. Chem. Lett., 4*, 2418−2422. https://doi.org/10.1021/jz401228c

10 Jurow, M., Schuckman, A.E., Batteas, J.D. & Drain, C.M. (2010). Porphyrins as molecular electronic components of functional devices. *Coord. Chem. Rev., 254*, 2297–2310. doi: 10.1016/j.ccr.2010.05.014

11 Collins, H.A., Khurana, M., Moriyama, E.H., Mariampillai, A., Dahlstedt, E., Balaz, M., Kuimova, M.K., Drobizhev, M., Yang, V.X.D., Phillips, D., Rebane, A., Wilson, B.C. & Anderson, H.L. (2008). Blood-Vessel Closure Using Photosensitizers Engineered for Two-Photon Excitation. *Nat. Photonics, 2*, 420–424. doi:10.1038/nphoton.2008.100

12 Smith, S.M., Markevitch, A.N., Romanov, D.A., Li, X., Levis, R.J. & Schlegel, H.B. (2004). Static and Dynamic Polarizabilities of Conjugated Molecules and Their Cations. *J. Phys. Chem. A, 108*, 11063–11072. https://doi.org/10.1021/jp048864k

13 Woller, T., Geerlings, P., De Proft, F., Champagne, B. & Alonso, M. (2019). Fingerprint of Aromaticity and Molecular Topology on the Photophysical Properties of Octaphyrins. *J. Phys. Chem., 123*, 7318–7335. https://doi.org/10.1021/acs.jpcc.8b10908

14 Woller, T., Geerlings, P., De Proft, F., Champagne, B. & Alonso, M. (2018). Aromaticity as a Guiding Concept for Spectroscopic Features and Nonlinear Optical Properties of Porphyrinoids. *Molecules, 23*, 1333. DOI: 10.3390/molecules23061333

15 Lim, J.M., Yoon, Z.S., Shin, J.-Y., Kim, K.S., Yoon, M.-Ch. & Kim, D. (2008). The Photophysical Properties of Expanded Porphyrins: Relationships Between Aromaticity, Molecular Geometry and Non-linear Optical Properties. *Chem. Commun., 45*, 261–273. https://doi.org/10.1039/B810718A

16 Schulz, S., Wong, R.J., Vreman, H.J. & Stevenson, D.K. (2012). Metalloporphyrins — an Update. *Front Pharmacol, 3*, 36. DOI: 10.3389/fphar.2012.00068

17 Strianese, M., Pappalardo, D., Mazzeo, M., Lamberti, M. & Pellecchia, C. (2021). The Contribution of Metalloporphyrin Complexes in Molecular Sensing and in Sustainable Polymerization Processes: a New and Unique Perspective. *Dalton Trans., 50*, 7898–7916. https://doi.org/10.1039/D1DT00841B

18 Simkowa, I., Latos-Graz˙yn´ski, L. & Stępień, M. (2010). *π* Conjugation Transmitted across a d-Electron Metallocene in Ferrocenothiaporphyrin Macrocycles. *Angew Chem Int Ed Engl., 49*, 7665–7669. https://doi.org/10.1002/anie.201004015

19 Simkowa, I., Latos-Graz˙yn´ski, L. & Stępień, M. (2013). Ruthenocenoporphyrinoids: Conformation Determines Macrocyclic *π*-Conjugation Transmitted Across a d-Electron Metallocene. *Angew Chem Int Ed Engl., 52*, 1044–1048. https://doi.org/10.1002/anie.201208289

20 Valiev, R.R., Kurten, T., Valiulina, L.I., Ketkov, S.Yu., Cherepanov, V.N., Dimitrova, M. & Sundholm, D. (2022). Magnetically Induced Ring Currents in Metallocenothiaporphyrins. *Phys. Chem. Chem. Phys., 24*, 1666–1674. https://doi.org/10.1039/D1CP04779E

21 Becke, A.D. (1988). Density-Functional Exchange-Energy Approximation with Correct Asymptotic Behavior. *Physical Review A., 38*, 3098–3100. https://doi.org/10.1103/PhysRevA.38.3098

22 Lee, C., Yang, W. & Parr, R.G. (1988). Development of the Colle-Salvetti Correlation-Energy Formula into a Functional of the Electron Density. *Phys. Rev. B: Condens. Matter Mater. Phys., 37*, 785–789. https://doi.org/10.1103/PhysRevB.37.785

23 Weigend, F. & Ahlrichs, R. (2005). Balanced Basis Sets of Split Valence, Triple Zeta Valence and Quadruple Zeta Valence Quality for H to Rn: Design and Assessment of Accuracy. *Phys. Chem. Chem. Phys., 7*, 3297–3305. https://doi.org/10.1039/B508541A

24 Gaussian 09, Revision A.02, Frisch, M.J., Trucks, G.W., Schlegel, H.B., Scuseria, G.E., Robb, M.A., Cheeseman, J.R. et al. (2016). Gaussian, Inc., Wallingford CT.

25 Fliegl, H., Taubert, S., Lehtonen, O. & Sundholm, D. (2011). The Gauge Including Magnetically Induced Current Method. *Phys. Chem. Chem. Phys., 13*, 20500–20518. https://doi.org/10.1039/C1CP21812C

26 Sundholm, D., Fliegl, H. & Berger, R. (2016). Calculations of Magnetically Induced Current Densities: Theory and Applications. *Wiley Interdiscip. Rev.: Comput. Mol. Sci., 6*, 639–678. https://doi.org/10.1002/wcms.1270

27 Gershoni-Poranne, R., Rahalkar, A.P. & Stanger, A. (2018). The Predictive Power of Aromaticity: Quantitative Correlation Between Aromaticity and Ionization Potentials and HOMO–LUMO Gaps in Oligomers of Benzene, Pyrrole, Furan, and Thiophene. *Phys. Chem. Chem. Phys., 20*, 14808–14817. https://doi.org/10.1039/C8CP02162G

28 Ashraf Janjua, M.R.S., Mahmood, A., Nazar, M.F., Yang, Z. & Pan, Sh. (2014). Electronic Absorption Spectra and Nonlinear Optical Properties of Ruthenium Acetylide Complexes: A DFT Study Toward the Designing of New High NLO Response Compounds. *Acta Chim Slov, 61*, 382–390.

29 Lim, I.S. (2004). Static Electric Dipole Polarizabilities of Atoms and Molecules (Doctoral dissertation). Retrieved from Massey University. (2010-09-27T00:15:35Z) http://hdl.handle.net/10179/1694

30 Cho, S., Yoon, Z.S., Kim, K.S., Yoon, M.-Ch., Cho, D.-G., Sessler, J.L. & Kim, D. (2010). Defining Spectroscopic Features of Heteroannulenic Antiaromatic Porphyrinoids, *J. Phys. Chem. Lett., 1*, 895–900. https://doi.org/10.1021/jz100039n

31 Valiev R.R., Fliegl, H. & Sundholm, D. (2017). Optical and Magnetic Properties of Antiaromatic Porphyrinoids. *Phys. Chem. Chem. Phys., 19*, 25979–25988. https://doi.org/10.1039/C7CP05460B

32 Padilla, W.J., Basov, D.N. & Smith, D.R. (2006). Negative refractive index metamaterials, *Materials Today, 9*, 28–35. https://doi.org/10.1016/S1369-7021(06)71573-5

Information about authors*

Valiulina, Lenara Ilmirovna — 1st year PhD student, Department of Optics and Spectroscopy, National Research Tomsk State University, Lenin Avenue, 36, 634050, Tomsk, Russia; e-mail: valiulina-lenara@mail.ru; https://orcid.org/0000-0002-3364-0448

Cherepanov, Victor Nikolaevich — Doctor of Physics and Mathematics, Head of Department of Optics and Spectroscopy National Research Tomsk State University, Lenin Avenue, 36, 634050, Tomsk, Russia; e-mail: vnch1626@mail.ru; https://orcid.org/0000-0002-5952-5202

Valiev, Rashid Rinatovich (*corresponding author*) — Doctor of Chemical Sciences, Assistant professor, National Research Tomsk State University, Lenin Avenue, 36, 634050, Tomsk, Russia; e-mail: valiev-rashid@mail.ru; http://orcid.org/0000-0002-2088-2608

*The author's name is presented in the order: *Last Name, First and Middle Names*